
Proceedings Paper:
Lockwood, APG, Kok Shun, P, Warren, NJ orcid.org/0000-0002-8298-1417 et al. (5 more authors) (2019) Dissolved Air Flotation for Rapid Dewatering and Separation of Legacy Sludge Wastes. In: Proceedings of the 2019 Waste Management Conference. Waste Management 2019, 03-07 Mar 2019, Phoenix Arizona. WM Symposia .

Dissolved Air Flotation for Rapid Dewatering and Separation of Legacy Sludge Wastes - 19065

Alexander P. G. Lockwood*, Philip Kok Shun*, Nicholas J. Warren*, Jeffrey Peakall**, Martyn Barnes***, Geoff Randall***, David Harbottle*, Timothy N. Hunter*
School of Chemical and Process Engineering, University of Leeds*
School of Earth and Environment, University of Leeds**
Sellafield Ltd***

ABSTRACT

As a low footprint, high efficiency separation process, Dissolved Air Floatation (DAF) could effectively be retrofitted into existing waste management facilities at nuclear sites such Sellafield and Hanford to rapidly separate particulates from aqueous suspensions. The simplicity (no moving parts) and size of this technology coupled with low cost of construction and reagent purchase would also be ideal for ease of facility decommissioning with minimum impact to secondary waste generation. For this study, methyl isobutyl carbinol (MIBC) was used in this research as a frothing agent to produce a preferable stable foam. $Mg(OH)_2$ was selected as a test material as it is the result of long term corrosion of Magnox fuel in UK nuclear fuel storage ponds. Due to the cationic nature of the $Mg(OH)_2$ test material, the anionic surfactant, Sodium Dodecyl Sulphate (SDS) was used as collector to modify the surface properties to increase hydrophobicity. The performance of anionic SDS in floating 2.5%*v/v* $Mg(OH)_2$ was compared to the adsorption isotherm of SDS on $Mg(OH)_2$ to determine monolayer coverage surfactant dose which was investigated using Total Organic Carbon (TOC). SDS was found to increase particulate recovery to 93% with some water carry-over observed and it was found that particle bubble attachment was optimum for a select particle size distribution. This study proved that potential application of flotation as an efficient viable dewatering technique for common magnesium hydroxide based legacy wastes, using cheap, readily available collector and frother agents.

INTRODUCTION

There are two major legacy ponds at the Sellafield site, the Pile Fuel Storage Pond (PFSP) and the First-Generation Magnox Storage Pond (FGMSP). These facilities were constructed in 1949 and 1962 respectively as open-air structures designed to receive and store irradiated fuel from Windscale Pile and Magnox reactors, and to de-clad fuel rods prior to the fuel being processed. PFSP ceased operating in 1962 though waste was still imported into the mid-70s and FGMSP accepted fuel until 1992[1], [2].

After a long storage period and being placed into a passive care and maintenance regime, the fuel rods, primarily their cladding, which comprises predominantly of Magnox, started corroding in the pond forming magnesium hydroxide. This gave rise to increased radiation levels from mobile soluble and particulate fuel rod fission products which also increase the turbidity of the pond water in addition to algae presence. These ponds have accumulated significant quantities of waste materials amongst the skips of fuel, including but not limited to large inventories of corroded Magnox sludge, fuel rod fragments, metal fragments (from fuel skips), concrete degradation products (from the pond infrastructure), wind-blown sand, and other materials such as bird guano and animal remains[2].

Some inventory has since been removed and placed in the Fuel Handling Plant (FHP), however, similar trends in activity to the legacy ponds have begun to be observed. Movement of containers with leaking fuel through the FHP pond and subsequent preparation of fuel for de-canning caused some activity to spread throughout the pond. The corrosion of the Magnox clad fuels increased activity levels in the FHP pond had from 200 $MBq.m^{-3}$ in 1990 to 6000 $MBqm^{-3}$ (2003). [3]

Decommissioning such facilities is extraordinarily difficult given complexities surrounding not just the complexity of heterogeneous chemically dynamic inventory, but also their location on site. The ponds are situated on a very congested part of the Sellafield site, surrounded by buildings which limits the opportunity for new infrastructure, heavy lifting and temporary facilities.

The ponds' infrastructures need to be maintained and improved whilst balancing time and money spent improving infrastructure against hazard reduction[4].

The current performance plan and 20-year review states that for PFSP retrievals and dewatering milestones shall be reached by 2030. However, FGMSP retrievals are currently planned to begin by 2050[5]. FGMSP will be dewatered as part of learning from experience (LFE) of the operational success of PFSP. There are significantly different challenges associated with FGMSP, as the activity levels are far greater (in the order of 1000 $TBq.m^{-3}$)[3] and there is significantly more sludge in the pond with PFSP approximately housing 300 m^3 and FGMSP housing approximately 1400 m^3 [6], [7].

Sellafield has initiated additional sludge retrieval (ASR) operations from FGMSP, which is an important milestone of the remediation programme. A dedicated facility called Sludge Packaging Plant (SPP1) was erected in 2013 costing £240 million which essentially consists of three 450 m^3 tanks, designed to collect sludge from FGMSP via sedimentation/settling, then return supernatant back to the FGMSP pond. At the start of the ASR project, SPP1 had been constructed and a pipe bridge was linking the facility to FGMSP. Slurry is sent to SPP1 in batches of 80 m^3 (including flushing of the slurry lined with pond water). Upon completion of sludge settling, the supernatant is returned to the FGMSP main pond via a dedicated coaxial pipe. [8].

The dewatering mechanism of SPP1, which is essentially a gravitational thickener or Secondary Settling Tank as used in the minerals and water treatment industries respectively, must account for the removal colloidal particulates. Under Stokesean settling mechanics, these particulates cannot be removed by settling as Brownian motion is sufficient to keep them suspended[9]. Removal of colloidal particulates, which are responsible for a multitude of engineering difficulties discussed below must be achieved with great haste. Gravitational settling is infamously slow, and is not the method of separation preferred by industry where low density differentials exist between particulate and suspension fluid or for systems contaminated with algae[10]. The density of coagulated $Mg(OH)_2$ has been investigated by Johnson *et al.*[11] was found to be 1059-1081 $kg.m^{-3}$. One technique that has been developed in the minerals industry to replace this archaic method for systems with low density differentials and high algae concentrations is floatation[10].

Maher *et al.*[12] linked increase in activity of discharges due to the fact that Site ion exchange plant (SIXEP) effluent streams contain amounts of suspended particles and colloids that could both interfere with the ion exchange process in SIXEP and act as a vector for the transport of radionuclides.

Colloids are known as potential controllers of radionuclide speciation and transport due to their small size and high surface area to mass ratio[12]. They are capable of binding radionuclides, particularly the actinides. Magnesium hydroxide particles have been reported to retain various radionuclides efficiently. The study by Maher *et al.* [12] showed that Pu(V) and Am(III) had strong sorption to larger brucite colloid particulates. Any radionuclides associated with larger particles should be most easily removed by the initial sand filtration column in SIXEP, and this is probably responsible for most of the removal of actinide activity from the feed solution. However, the sand bed filter will not remove all small colloids. It would be expected that a simple ion exchange column would be relatively ineffective at removing any radionuclides that were incorporated within colloids which may account for the rise in total alpha activity being discharged to the sea with the increasingly intensive retrieval operations occurring on site[12]–[14].

In 2011 Sellafield released the" Sellafield IWS Annual Progress Report "[15] which broke down discharges into groups associated with specific operations, i.e. reprocessing, legacy waste retrievals, ground remediation etc. The report indicates that whilst discharge activity are largely expected to drop after the THORP and Magnox reprocessing regimes cease by 2020 as discussed in the Nuclear Decommissioning Authority (NDA) Business Plan 2017-2020 [16], activity attributed to legacy activities will still contribute to liquid discharges to the Irish sea.

The largest contributors in 2011 from Legacy facilities in total activity were ^{3}H, ^{90}Sr, ^{99}Tc, ^{125}Sb, ^{137}Cs and ^{241}Pu with each having a total activity contributions of between 0.1TBq and 1.2TBq each[15].

These trends have continued to be reported up to 2016 [17], where a steady rise in total alpha and beta activity has been noted. Whilst reprocessing operations have intensified, contributions from legacy waste have also increased[17]. This rise in activity discharge has been linked to suspended particulates in effluent treatment facilities.

Floatation is a rapid dewatering technology developed in the 19th century that has been utilised by many industries, but most commonly found in the minerals industry, recycling of effluent, proteins, plastic wastes as well as the de-inking of waste paper and the extraction of residual oil from porous rock[18]. Floatation involves the separation of minerals from a suspension by differences in hydrophobicity. Typically the functional reagents in this process are referred to as[19]:

- Frothers: Typically organic, these materials, when dissolved in water, enables the system to form a more or less stable froth with air.
- Collectors: Typically organic, a material that when adsorbed to the surface of a mineral, reduces its hydrophilicity allowing the particle to be adsorbed at the water-air interface. In the presence of a frother, this may also create a more or less stable froth.
- Activators: Similar to collectors but are generally inorganic.
- Depressants: typically inorganic, this minerals will increase the hydrophobicity of select minerals in the suspension.

Frothers are usually aliphatic or cyclic alcohols such as Methyl-isobutyl-carbinol (MIBC) and α-terpineol, but polyglycol ethers such as 'Dow froth' can also be used. Gupta *et al.* [20] investigated the effects of these frothers on the floatation of coal. It was found that MIBC was the least surface active but the most effective frother, producing fine and monosized bubbles which were more effective at removing fine particles [20]. MIBC is a widely used frother [20]–[23] and has been selected as the frother for this floatation work.

Given the hydrophilicity surface charge of $Mg(OH)_2$, an anionic surfactant such as Sodium Dodecyl Sulphate (SDS) would likely be an appropriate collector. Therefore given its extensive investigation in other literature[18], it has been selected for preliminary investigation.

Floatation has been utilised in this industry for years, one of the major technological developments is the Jameson cell. Advantages of the Jameson cell are[24]:

- Consistent fine bubble generation with no external equipment or spargers.
- Intense mixing with small bubbles achieving rapid flotation without mechanical agitation.
- High throughput in a small footprint.
- Froth washing maximizes concentrate grade in a single flotation stage.
- Fast response and easy control.
- Steady operation and performance irrespective of changes in feed flow.
- No moving parts, simple to install and maintain, excellent availability.

Flotation is used extensively across minerals and water industries to selectively separate and rapidly de-water, but, to date, has not been extensively incorporated into nuclear waste separation operations. DAF technology is reported to have netted $38.6 Billion (Aus) in exports from Australia as per an independent report on the value of the Jameson Cell to the Australian economy 1990-2014 by Manford Pty Ltd Coal energy consultants[25]. The Cell has highly suitable characteristics for the nuclear industry provided the correct frother and collector is selected.

BACKGROUND

Adsorption Isotherm

The adsorption isotherm shown in equation 2, used in this research is the two step adsorption isotherm suggested by Zhu and Ghu[26], which as described by Brown and Zhao [27] adapted to the present framework regarding the Langmuir adsorption isotherm follows the following two step adsorption mechanism:

1) In a first non-cooperative step single surfactant molecule are adsorbed by hydrophobic interactions with the solid surface.
2) In the second cooperative step at higher surface coverage, surfactant molecules reorientate to expose the head groups to the solution and to optimize interactions between the alkyl chains with the formation of micelles or hemimicelles.

By mass action reasoning:

$$\Gamma = \frac{\Gamma_\infty k_1 C \left(\frac{1}{n} + k_2 C^{n-1}\right)}{1 + k_1 C(1 + k_2 C^{n-1})} \quad (2)$$

Where Γ is the amount of surfactant adsorbed at concentration C. Γ_∞ is the limiting adsorption (anion exchange capacity) at high concentrations, k_1 and k_2 are equilibrium constants involved at the first and second steps of adsorption respectively. Finally n is the aggregation number of surface hydrophobic aggregates [26]. In this paper, this isotherm model is used for SDS adsorption onto $Mg(OH)_2$.

Recovery Percentage ($R_\%$)

$$R_\% = \left(\frac{M_r}{M_T}\right) \times 100\% \quad (3)$$

The recovery percentage is shown in equation 3, where the recovery percentage, $R_\%$, from $Mg(OH)_2$ suspensions as suggested by Zhang *et al.* [28]is the percentage of the mass of $Mg(OH)_2$ recovered from the initial suspension in the foam phase and the total mass of $Mg(OH)_2$ prior to DAF operations. M_r is the recovered mass of $Mg(OH)_2$ from DAF operations and M_T is the total initial mass of $Mg(OH)_2$ in the system.

Residual Volumetric Concentration ($\xi_\%$)

$$\xi_\% = \frac{(M_T - M_r)/\,\rho_{Mg(OH)_2}}{V_T - V_r} \times 100\% \quad (4)$$

Derived from a material balance of the DAF, the residual volumetric concentration shown in equation 4, $\xi_\%$, is a function of the mass difference between the initial mass, M_T, and the recovered mass M_r. The residual mass is then divided by the density of $Mg(OH)_2$ (2344 $g.l^{-1}$) to compute a volume. This is then divided by the remaining volume in the system which is the difference between the initial volume, V_T, and the recovered volume of collapsed foam V_r.

Volume Reduction Factor (V_{red})

$$V_{red} = \left(\frac{V_T}{V_r}\right) \quad (5)$$

V_{red} is the volume reduction factor suggested by Mahmoud *et al.* [29]where V_T is the total volume of the suspension (210ml) and V_r is the volume of extracted suspension i.e. collapsed foam. A larger reduction factor with high floatation yield is favourable, as this means that a large number of particulates have been extracted whilst minimalizing the entrainment of fluid.

MATERIALS AND EXPERIMENTAL METHODOLOGY

$Mg(OH)_2$ (Versamag, Martin Marietta, US) was used for settling and aggregation experiments and was analysed using a Malvern Mastersizer 2000E (model no. EPA2000) to have a particle D[0.5] of 2.44 µm. Versamag is a fine white precipitated powder with a solubility of 6.9 $mg.l^{-1}$ in water[30].

Sodium Dodecyl Sulphate (SDS) pellets (TOKU_E ≥99%) were dissolved in 0.5 l of milliQ water to make up a bulk solution of 16.4 mM which was stored in a polypropylene container previously washed with Decon-90, then rinsed with ethanol to disperse any remaining surfactants, rinsed with milliQ water and dried in an oven to remove any moisture. This bulk solution was diluted with milliQ water accordingly for experiments.

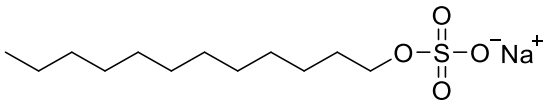

Figure 1: Chemical structure of sodium dodecyl sulphate.

A stock solution of 100 ppm concentration was made using 4-methyl-2-pentanol (MIBC) (Sigma-Aldrich, 98%, density: 0.802 $g.ml^{-1}$ and milliQ water. MIBC was used as a frothing agent for bubble stability and dissolved air floatation experiments[31].

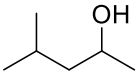

Figure 2: Chemical structure of methyl isobutyl carbinol.

Characterisation of material

$Mg(OH)_2$ was analysed using a Hitachi SU8230: high performance cold field emission Scanning Electron Microscope (SEM). The $Mg(OH)_2$ was coated by 10 nm of iridium to reduce charging effects before imaging. The volume average spherical equivalent diameter of $Mg(OH)_2$ in aqueous solution was found using a Malvern Mastersizer 2000E (Malvern, UK) by preparing a 2.5%v/v sample in milliQ water and dispensing aliquots from this stock solution into the Mastersizer dispersion unit until the concentration is within the equipment's obscuration limits. The specific surface area was determined using a Micormetrics Tristar 3000 (Micrometrics, Lincoln, UK) nitrogen BET isotherm method. The ζ-potential was established using a Malvern Zetasizer (Malvern UK) by sonicating and diluting a 2.5%v/v suspension of $Mg(OH)_2$ in milliQ water.

Adsorption Studies

Adsorption studies were completed using Total Organic Carbon (TOC) analysis. Samples were prepared in 15 ml sterile centrifuge tubes with 2.5%*v/v* $Mg(OH)_2$ particle concentration and varying amounts of SDS surfactant ranging from 4.1 $\mu mol.l^{-1}$ to 820 $\mu mol.l^{-1}$. Adsorption studies were limited at the upper bound of these concentrations due to concerns that SO_2 dissolution into H_2SO_4 upon combustion may damage the analytic equipment.

The particle-surfactant suspension was then agitated on a rotary tube agitator for 24 hours to ensure adsorption equilibrium was achieved. It was then placed in a centrifuge at 4×10^4 rpm for 20 minutes to sediment particles. An aliquot of the supernatant was taken using a 10 ml syringe and injected into a TOC sample vial through a syringe filter (0.45 µm pore size) to remove any trace particles.

The remaining surfactant was compared to two controls, samples of the same concertation surfactant systems without $Mg(OH)_2$ and a system containing just $Mg(OH)_2$ with centrifuged and filter supernatant to offset for any organic contamination. This adsorbed surfactant could then be established via material balance differential calculation.

The TOC analyser used was a Hach Lange IL550 (Hatch, United Kingdom). The TOC outputs total carbon and total inorganic carbon, resulting in the total organic carbon being determined through a material balance differential method. The Zu and Ghu model was fitted to the adsorption data using OriginPro 2018 via a Levenberg Marquardt iteration algorithm. Errors were calculated using propagation of uncertainty. I.e. for $C=f(a,b)$ then: the absolute error of c, Δc is shown in equation 5:

$$\Delta c = \sqrt{(\frac{\partial c}{\partial a})^2 \Delta a^2 + (\frac{\partial c}{\partial b})^2 \Delta b^2} \quad (5)$$

Dissolved Air Floatation particulate recovery

A bespoke floatation cell (210 ml, 65 mm ID; Figure 3) was manufactured with an air inlet and a fritted glass base. 12.31 g of $Mg(OH)_2$ was added to a measuring cylinder with 2.6ml of MIBC, the required dose of SDS and then made up to 210ml with milliQ water (98µM of MIBC). A sample of this suspension was then taken, placed into a preweighed aluminium tray, weighed and then placed into an oven for 24 hours to confirm the solids content due to heterogeneity of the bulk solution. The cell of was agitated with an overhead stirrer for 20 minutes at 250 rpm to allow adequate mixing and adsorption of SDS to $Mg(OH)_2$ surfaces. Once the mixing phase was complete flow into the bottom of the cell was set at 0.1 $l.min^{-1}$ and the agitator speed was reduced to 100 rpm to suspend larger particulates but minimise turbulence in the cell. Foam generated above the air water interface would then pour through the outlet at the top of the vessel and into a reweighed aluminium container. This container was then placed into an oven for 24 hours to evaporate the water component of the foam, leaving behind the recovered particulates which were then weighed to determine recovery efficiency via equation 3 and the residual particulate concentration by equation 4.

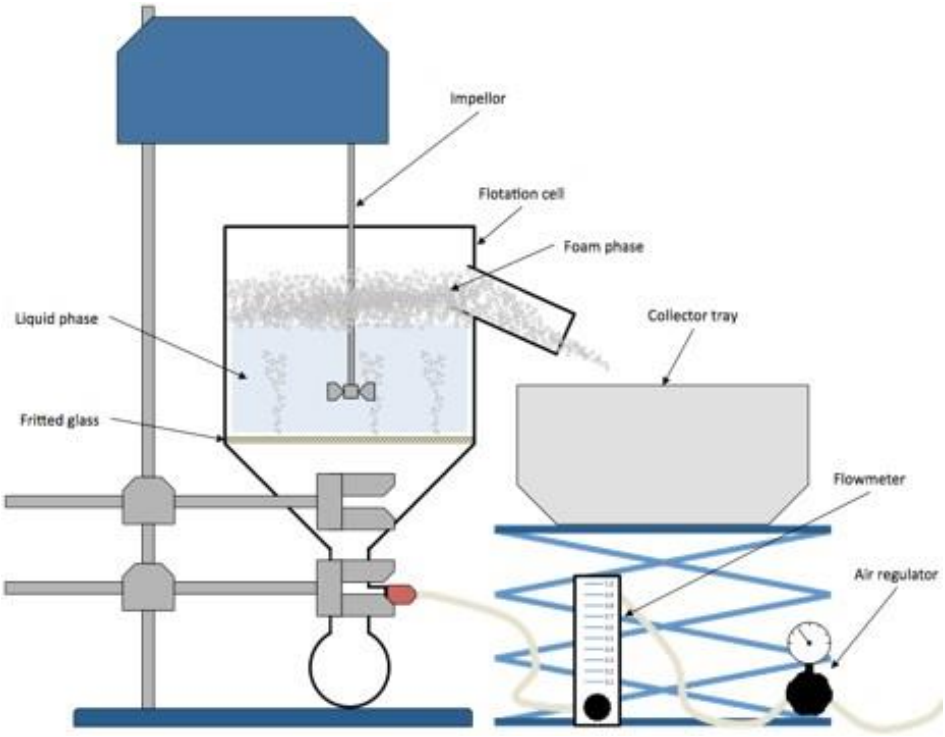

Figure 3: Experimental set-up used for DAF studies

RESULTS AND DISCUSSION

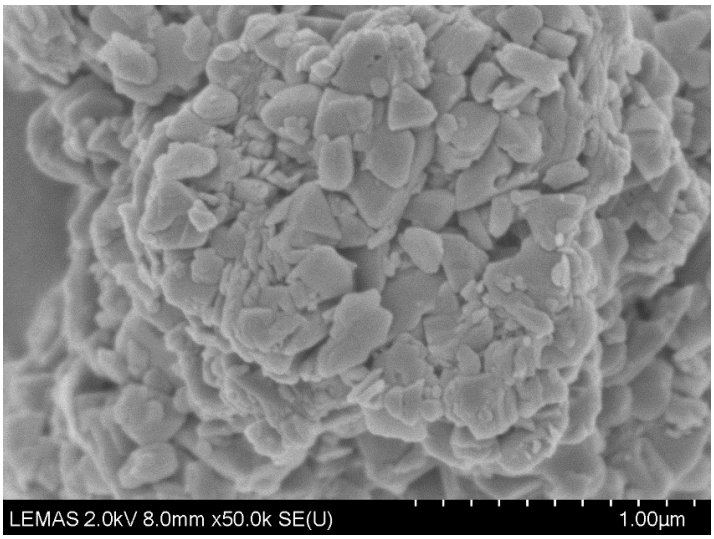

Figure 4: Scanning electron micrograph of dry $Mg(OH)_2$ particles coated in 10nm Iridium.

Figure 4 shows a scanning electron micrograph of $Mg(OH)_2$ revealing that $Mg(OH)_2$ is made up of aggregates of pseudo-hexagonal platelets similar to those reported by Johnson *et al.* [11] and Maher *et al.*[12]. EDX showed that the $Mg(OH)_2$ sample was primarily Mg and O with small amounts of Ca and Cl impurities again similar to those reported by Johnson *et al.*[11] as a likely result of the versamag manufacturing process. Table 1 shows a summary of the $Mg(OH)_2$ material properties such as the D[0.5], the ζ-potential, the BET specific surface area and the pH of the 2.5%v/v $Mg(OH)_2$ suspension.

Table 1: Physical characteristics of $Mg(OH)_2$ suspended in MilliQ water at 2.5% v/v.

Species	**D[0.5](µm)**	**ζ-Potential (mV)**	**BET S.A. (m^2g^{-1})**	**pH**
$Mg(OH)_2$	2.45 ± 0.31	12.03 ± 0.03	7.56 ± 0.17	10.10 ± 0.26

The volume average spherical equivalent diameter of $Mg(OH)_2$ in aqueous solution was found to be 2.45 ± 0.31 µm (after sonification, this material naturally coagulates to form larger aggregates as observed by Johnson *et al.* [11]who observed similar coagulation using similar material) indicating that the lower particle sizes may not be compatible with floatation which is generally estimated as being between 20-100 µm diameter. $Mg(OH)_2$ has a specific surface area of 7.56 ± 0.17 $m^2.g^{-1}$, whilst high, Biggs *et al.*[32] have observed similar $Mg(OH)_2$ material as having a specific surface area of 15.43 $m^2.g^{-1}$.This is expected of aggregated material due to its fractal nature and high porosity[33]. Similar pseudo-hexagonal platelet material such as aluminium hydroxide, has been found to have similarly high surface area, these BET surface areas range from 1.5 $m^2.g^{-1}$ as observed by Adekola *et al.* up to 91 $m^2.g^{-1}$ observed by Rovenqvist[34]. Due to the self-buffering properties of $Mg(OH)_2$, a function of $Mg(OH)_2$ semi solubility in water observed by Johnson et al. [11], the ζ-potential was found to be 12.03 ± 0.03mV at a pH of 10.10 ± 0.26. This agreed with previous studies of $Mg(OH)_2$ barring the slightly higher surface charge than those reported by Johnson *et al.*[11] and Biggs *et al.* [32] for similar material.

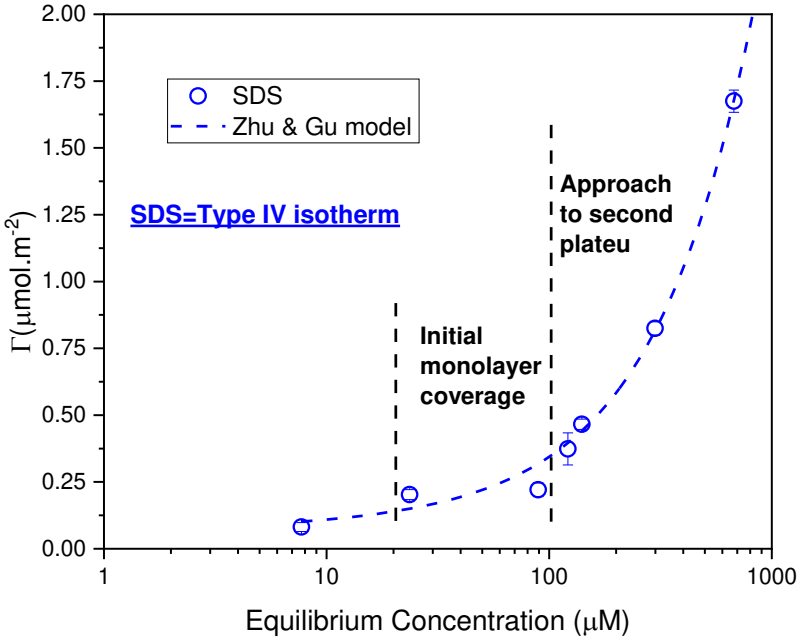

Figure 5: Comparison of adsorption isotherms describing adsorption mechanism to the surface of 2.5%v/v $Mg(OH)_2$. The Zhu et al bilayer adsorption isotherm fitted to the SDS data had a coefficient of determination of 0.9911.

Figure 5 shows the effect on equilibrium concentration of SDS on the amount of SDS adsorbed onto the $Mg(OH)_2$ surface adsorption mechanism of SDS to the surface of $Mg(OH)_2$. The occurrence of the monolayer coverage in the 20-100 μM region indicates the concentration range at which the SDS dose is most effective. Excess SDS in the system will tend towards the air-water interface lowering the surface tension of the water and increasing foamability[18]. In the first stage, the single surfactant molecules are adsorbed by hydrophobic interactions with the solid surface to form a monolayer, in this case, the sulphate head group of SDS on the $Mg(OH)_2$ surface, as per the Zhu and Gu model.

The Zu and Ghu model was fitted to the adsorption data and had a coefficient of determination of 0.9911. The equilibrium constant of this first monolayer adsorption stage, k_1, was found to be 3.08 x 10^{-5} l.μmol^{-1} as shown in table 2. This suggest that very little SDS is required in relation to the equilibrium concentration to produce a monolayer on $Mg(OH)_2$ as this value describes the first plateau event on the isotherm as shown in figure 5 given by the theory developed by Zhu and Gu[26]. In a study by Brown and Zhao[27] on the adsorption of SDS polystyrene latex this first equilibrium constant, k_1, was found to be 1.0 x 10^3, the system investigated produced a ζ-potential of -27 mV and a D[0.5] of 202 μm. The fist plateau occurs at a $\Gamma/\Gamma\infty$ ratio of ≈0.1 which was like the value of 0.023 determined in the TOC adsorption experiment. For floatation, this first plateau is important as the monolayer coverage region is where hydrophobicity is at its maximum[35].

Table 2: Summary of adsorption isotherm fitting data for the Zhu and Gu model adsorption isotherms.

Property	SDS Value
Γ_∞ (μmol.l^{-1})	8.77
K_1 (l.μmol^{-1})	3.08x10^{-5}
K_2 (l.μmol^{-1})	247.46
n (dimensionless)	0.11
Γ/Γ_∞ monolayer	0.023

The second stage of SDS adsorption to $Mg(OH)_2$ comprises of the orientation of SDS so that the hydrophobic tales form a bilayer to reduce the free energy of the surface further[26]. The second stage equilibrium constant, k_2, with a value of 247.46 $l.\mu mol^{-1}$ is far greater than the value for the first equilibrium constant which is sound logic regarding the physical system, as far less surfactant molecules are required to form a monolayer than a bilayer, which agrees with the observation for the large gap between the first and second adsorption plateau observed in literature by Zhao and Brown[27] in their investigation of SDS adsorption in to latex observing a value of 2 x 10^9 and is part of the theory developed by Zhu and Gu[26].

The monolayer aggregation number (effectively a surfactant head group packing density) is very low for this physical system. However as this is not a complete data set as the second plateau was not observed within the operating limits of the technique, this value is likely larger. This is observed by Somasundaran and Fuerstenau [36]who found that the second plateau for SDS on $15m^2.g^{-1}$ alumina was around 4 $\mu mol.m^{-2}$ adsorption concentration[36], [37]. A value of 3.3 $\mu mol.m^{-2}$ for the second plateau indicating bilayer formation was observed by Gao and Chorover[38] when investigating the adsorption of SDS on hematite, suggesting that the investigatory scope of this technique should be extended. Other literature has observed monolayer aggregation numbers in the region of 3-24 and is often dependent on head group repulsion on the surface and chain length[39].

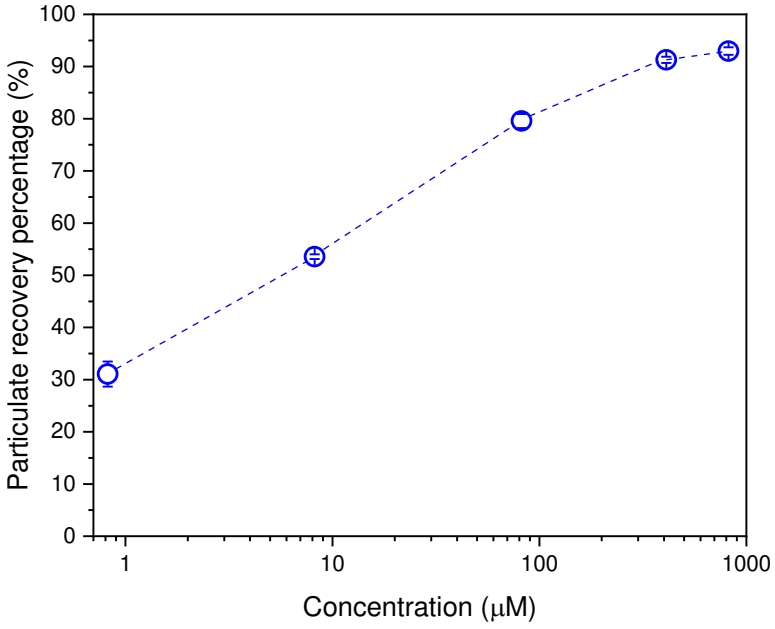

Figure 6a: Recovery percentages of varying concentrations of SDS surfactant as a hydrophobic surface modifier on 2.5%v/v $Mg(OH)_2$ suspensions. Line added as a guide for the eye only.

Floatation of $Mg(OH)_2$ using SDS as a hydrophobic surface modifier proved to be effective. Achieving as much as 93% recovery of $Mg(OH)_2$ calculated using equation 3 as shown in figure 6a. However, the effectiveness of such extraction (for the purposes of rapid dewatering) cannot be measured solely as a function of recovery, as the remaining supernatant concentration (shown in figure 6b: a measure of the remaining particulate concentration in suspension described by equation 4) and volume reduction (see figure 6c: a ratio of volume of fluid removed against the initial concentration described in equation 5) must also be considered. Flocculation is limited by particle size as fine particles are generally difficult to treat in dissolved air flotation due to bubble streamline effects, the difficulty in draining the film between the particle/bubble and especially due to fines entrainment[40].

There is evidence that fines entrainment in this system may be occurring as at concentrations above monolayer formation (figure 5) where recovery is observed to increase, even though the particles should not be strongly hydrophobic at that point due to the bi-layer formation (with the negative surfactant head groups facing the aqueous phase). This increase in recovery is likely therefore to be linked to the increased entrainment of particles as a result of excess SDS increasing foamability of the suspension reducing the system volume reduction factor[29].

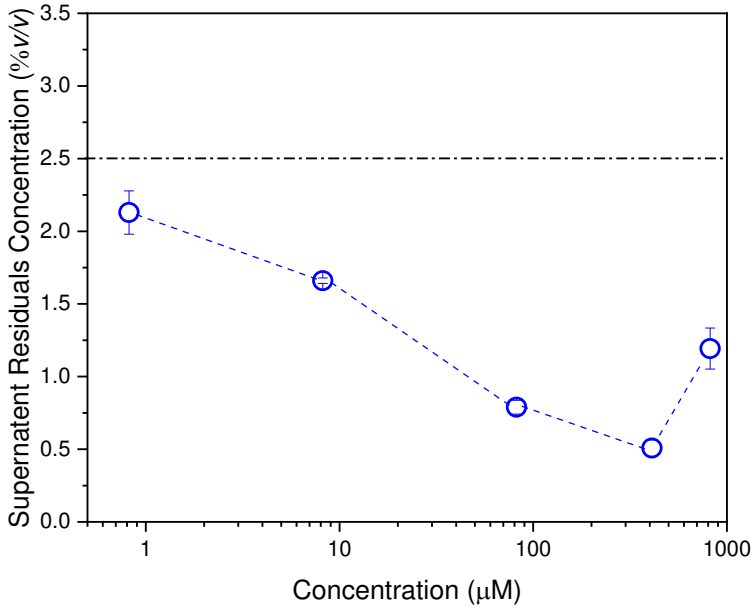

Figure 6b: Effect on suspension concentration of varying concentrations of SDS surfactant as a hydrophobic surface modifier on 2.5%v/v $Mg(OH)_2$ suspensions. Line added as a guide for the eye only.

The balance of fluid carry-over to particle extraction can be seen to become less effective at 820 μM SDS dose when the residual supernatant concentration begins to increase. This is likely a function of increased surface excess SDS lowering surface tension at the air water interface driving foamability[18]. This also indicates the start of bilayer formation reducing the hydrophobicity by orientating the hydrophilic sulphur head group out to the bulk suspension reducing the necessity for water dipole reorientation, therefore increasing entropy which axiomatically decreases the system free energy and, by result, the extractability of the particulates[27], [39].

The system can likely be optimised by adhering to SDS dose that results in monolayer formation with minimum SDS excess and by varying the frother (MIBC) concentration which is held at 98 μM for this study. Alteration of the frother concertation will control fluid carry over and entrainment of fines[20]. Additionally, in industry, given the effect of the particle size distribution on particle extractability (the maximum size of floating particles depends on their size, density, hydrophobicity, dynamics of the process which for a Jameson cell is typically 20-150 μm[41]–[43]) it is becoming more regular that these processes include a flocculation phase, either as suggested by Bunker *et al.* [44] via coagulation i.e. alum, ferric salts or polyaluminium chlorides on aquatic humic and non-aquatic humic waters or more recently, the development of pH and temperature responsive polymers (anionic in this case). These polymers can be tailored to flocculate then hydrophobize fine hydrophilic particles such as poly(N-isopropyl acrylamide)-poly(acrylic acid) and poly(N-isopropyl acrylamide)-poly(ethyl xanthate methacrylate) copolymers which require varying doses typically in the region of 50-1000 $g.t^{-1}$ depending on the properties of the floating material[40], [45].

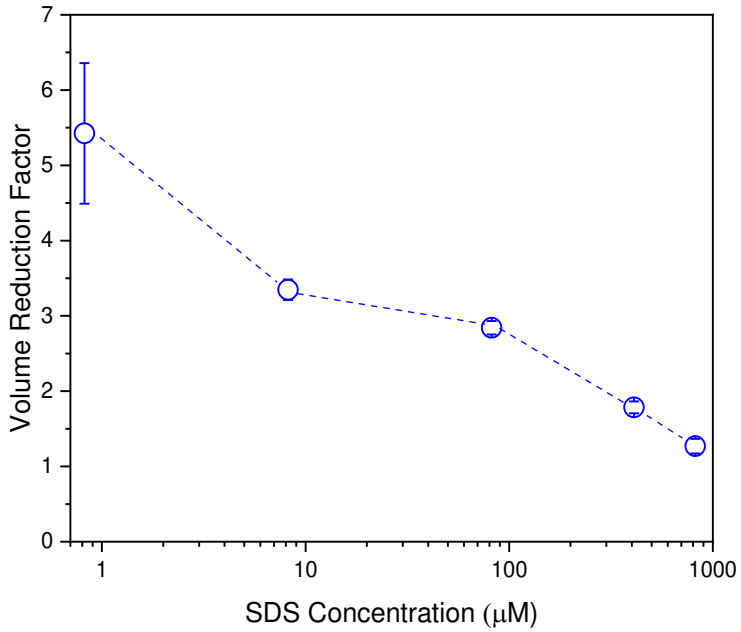

Figure 6c: Effect on volume reduction factor for varying concentrations of SDS surfactant as a hydrophobic surface modifier on 2.5%v/v $Mg(OH)_2$ suspensions. Line added as a guide for the eye only.

CONCLUSION

In summary, the application of dissolved air floatation for rapid dewatering and separation of legacy waste suspensions is a sparse area of research with great potential. Given the surface charge properties of the suspended $Mg(OH)_2$ in Sellafield's First-Generation Magnox Storage pond, an anionic surfactant such as sodium dodecyl sulphate can be used for rapid extraction. The technology can not only produce as much as 93% extracted material unoptimized but the application of the technology such as the Jameson Cell also addresses UK nuclear specific issues such as the need for low geometric footprint, no moving parts, simple maintenance to reduce worker dose and steady operation and performance irrespective of changes in feed flow. Optimisation of this system involves variation of frother agent concentration and air flow rate for a desired particle concentration (2.5*%v/v)* which are simple to achieve on a pilot scale as optimum collector dose can be established by simple adsorption studies to determine monolayer development concentration found in this paper to be in the range of 20-100 μM. Flotation can be adapted to improve fines extraction by addition of a flocculation/coagulation stage prior to floatation to increase fine particle size and prevent particle-bubble attachment being inhibited by bubble rise path slipstreams.

REFERENCES

[1] RWMD, "Packaging of Encapsulation of Legacy Fuel and Fuel Bearing Materials from Sellafield Ponds (Conceptual stage) Summary of Assessment Report," 2011. [Online]. Available: https://rwm.nda.gov.uk/publication/encapsulation-of-legacy-fuel-and-fuel-bearing-materials-from-sellafield-ponds/.

[2] S. F. Jackson, S. D. Monk, and Z. Riaz, "An investigation towards real time dose rate monitoring, and fuel rod detection in a First Generation Magnox Storage Pond (FGMSP)," *Appl. Radiat. Isot.*, vol. 94, pp. 254–259, Dec. 2014.

[3] A. Richardson and P. Maher, "Sellafield Fuel Handling Plant Pondwater update NuSAC(04)P17. (Update of NuSAC(03)P10)," 2004. [Online]. Available: http://www.hse.gov.uk/aboutus/meetings/iacs/nusac/051104/p10.pdf. [Accessed: 16-Jun-2018].

[4] Nuclear Decommissioing Authority, "Packaging of Encapsulation of Legacy Fuel and Fuel Bearing Materials from Sellafield Ponds (Conceptual Stage)," 2012. [Online]. Available: https://rwm.nda.gov.uk/publication/encapsulation-of-legacy-fuel-and-fuel-bearing-materials-from-sellafield-ponds/?download.

[5] NDA, "Nuclear Decommissioning Authority - GOV.UK," 2018. [Online]. Available: https://www.gov.uk/government/organisations/nuclear-decommissioning-authority. [Accessed: 03-May-2018].

[6] P. G. Heath, M. W. A. Stewart, S. Moricca, and N. C. Hyatt, "Hot-isostatically pressed wasteforms for Magnox sludge immobilisation," *J. Nucl. Mater.*, vol. 499, pp. 233–241, Feb. 2018.

[7] S. T. Barlow, M. C. Stennett, R. J. Hand, S. P. Morgan, and N. C. Hyatt, "Thermal Treatment of UK Magnox Sludge," in *2nd Petrus-OPERA PhD and early stage researcher conference 2016* , 2016.

[8] I. Grant, U. Weintrager, I. E. Richardson, and D. Wilson, "Sellafield FGMSP Additional Sludge Retrievals A Significant Step in Decommissioning Part of the U.K.'s Nuclear Legacy - 16180," in *Waste Management Symposium*, 2016.

[9] D. J. Shaw, *Introduction to Colloid and Surface Chemistry*. Butterworth-Heinemann, 1992.

[10] M. R. Teixeira and M. J. Rosa, "Comparing dissolved air flotation and conventional sedimentation to remove cyanobacterial cells of Microcystis aeruginosa: Part I: The key operating conditions," *Sep. Purif. Technol.*, vol. 52, no. 1, pp. 84–94, Nov. 2006.

[11] M. Johnson, J. Peakall, M. Fairweather, S. Biggs, D. Harbottle, and T. N. Hunter, "Characterization of Multiple Hindered Settling Regimes in Aggregated Mineral Suspensions," *I&EC Res.*, vol. 55, pp. 9983–9993, 2016.

[12] Z. Maher *et al.*, "Americium and plutonium association with magnesium hydroxide colloids in alkaline nuclear industry process environments," *J. Nucl. Mater.*, vol. 468, pp. 84–96, Jan. 2016.

[13] Z. Maher *et al.*, "Colloidal Processes in SIXEP Streams Introduction (1)," in *NNL Technical Conference*, 2015.

[14] Z. Maher, "Actinide Abatement in SIXEP," *NNL Technical Conference*, 2014. [Online]. Available: http://www.nnl.co.uk/media/1590/nnl-tech-conference-presentation-zoe-maher-sixep-may-14.pdf. [Accessed: 05-Sep-2017].

[15] Sellafield Ltd., "Sellafield Integrated Waste Strategy (IWS) Progress Report," 2011. [Online]. Available: http://www.cumbria.gov.uk/eLibrary/Content/Internet/538/755/2146/40927113059.pdf. [Accessed: 18-Jun-2018].

[16] Nuclear Decommissioning Authority, "Business Plan 2017 to 2020," 2017. [Online]. Available: http://namrc.co.uk/wp-content/uploads/2017/04/NDA_Business_Plan_2017_to_2020.pdf. [Accessed: 18-Jun-2018].

[17] Sellafield Ltd, "Discharges and Environmental Monitoring," 2016. [Online]. Available: https://www.gov.uk/government/uploads/system/uploads/attachment_data/file/658749/Monitoring_Environmental_Discharges_2016_FINAL.pdf. [Accessed: 28-Feb-2018].

[18] R. J. Pugh, *Bubble and foam chemistry*. Cambridge, 2016.

[19] C. C. Dewitt, "Froth Flotation Concentration," *Sep. Oper.*, pp. 652–658, 1940.

[20] A. K. Gupta, P. K. Banerjee, A. Mishra, P. Satish, and Pradip, "Effect of alcohol and polyglycol ether frothers on foam stability, bubble size and coal flotation," *Int. J. Miner. Process.*, vol. 82, no. 3, pp. 126–137, Apr. 2007.

[21] F. Melo and J. S. Laskowski, "Fundamental properties of flotation frothers and their effect on flotation," *Miner. Eng.*, vol. 19, no. 6–8, pp. 766–773, May 2006.

[22] T. N. Hunter, E. J. Wanless, and G. J. Jameson, "Effect of esterically bonded agents on the monolayer structure and foamability of nano-silica," *Colloids Surfaces A Physicochem. Eng. Asp.*, vol. 334, no. 1–3, pp. 181–190, Feb. 2009.

[23] J. S. Laskowski, Y. S. Cho, and K. Ding, "Effect of Frothers on Bubble Size and Foam Stability in Potash Ore Flotation Systems," *Can. J. Chem. Eng.*, vol. 81, no. 1, pp. 63–69, May 2008.

[24] G. Harbort, S. De Bono, D. Carr, and V. Lawson, "Jameson Cell fundamentals—a revised perspective," *Miner. Eng.*, vol. 16, no. 11, pp. 1091–1101, Nov. 2003.

[25] E. D, Osborne, J, "Independent Report Value of the Jameson Cell to the Australian Economy Contents," Wellington point, Australia, 2015.

[26] B.-Y. Zhu and T. Gu, "General Isotherm Equation for Adsorption of Surfactants at Solid/ Liquid Interfaces Part 1. Theoretical," 1989.

[27] W. Brown and J. Zhao, "Adsorption of sodium dodecyl sulfate on polystyrene latex particles using dynamic light scattering and zeta potential measurements," *Macromolecules*, vol. 26, no. 11, pp. 2711–2715, May 1993.

[28] H. Zhang, Y. K. Kim, T. N. Hunter, A. P. Brown, J. W. Lee, and D. Harbottle, "Organically modified clay with potassium copper hexacyanoferrate for enhanced Cs^+ adsorption capacity and selective recovery by flotation," *J. Mater. Chem. A*, vol. 5, no. 29, pp. 15130–15143, 2017.

[29] M. R. Mahmoud, M. A. Soliman, and G. M. Rashad, "Performance appraisal of foam separation technology for removal of Co(II)-EDTA complexes intercalated into in-situ formed Mg-Al layered double hydroxide from radioactive liquid waste," 2017.

[30] "Versamag Mg(OH)2 MSDS," no. CAS # 1309-42-8. Martin Marietta Magnesia Specialties, 2016.

[31] IXOM, "Methyl Isobutyl Carbinol MSDS," 2017.

[32] S. Biggs, R. Nabi, C. Poole, and A. Patel, "The Influence of Zeta Potential and Yield Stress on the Filtration Characteristics of a Magnesium Hydroxide Simulant," in *11th International Conference on Environmental Remediation and Radioactive Waste Management, Parts A and B*, 2007, pp. 1133–1139.

[33] S. M. Glover, Y. Yan, G. J. Jameson, and S. Biggs, "Bridging flocculation studied by light scattering and settling," *Chem. Eng. J.*, vol. 80, no. 1–3, pp. 3–12, Dec. 2000.

[34] J. Rosenqvist, "Surface chemistry of Al and Si (hydr)oxides, with emphasis on nano-sized gibbsite (α-Al(OH) 3)," Department of Chemistry, Inorganic chemistry Umea University, Sweeden, 2002.

[35] S. R. Rao and J. Leja, *Surface chemistry of froth flotation. Volume 1, Fundamentals.* .

[36] P. Somasundaran and D. W. Fuerstenau, "Mechanisms of Alkyl Sulfonate Adsorption at the

Alumina-Water Interface," *J. Phys. Chem.*, vol. 70, no. 1, pp. 90–96, Jan. 1966.

[37] D. Quijada, Lugo. Merileth, "Adsorption of Surfactants on Colloidal Silica: Effects of Surface Curvature on the Structure of Surface Aggregates," Technische Universität Berlin, 2010.

[38] X. Gao and J. Chorover, "Adsorption of sodium dodecyl sulfate (SDS) at ZnSe and α-Fe2O3 surfaces: Combining infrared spectroscopy and batch uptake studies," *J. Colloid Interface Sci.*, vol. 348, no. 1, pp. 167–176, Aug. 2010.

[39] H. Rupprecht and T. Gu, "Structure of adsorption layers of ionic surfactants at the solid/liquid interface," *Colloid Polym. Sci.*, vol. 269, no. 5, pp. 506–522, May 1991.

[40] W. S. Ng, L. A. Connal, E. Forbes, and G. V. Franks, "A review of temperature-responsive polymers as novel reagents for solid-liquid separation and froth flotation of minerals," *Miner. Eng.*, vol. 123, pp. 144–159, Jul. 2018.

[41] A. Norori-McCormac, P. R. Brito-Parada, K. Hadler, K. Cole, and J. J. Cilliers, "The effect of particle size distribution on froth stability in flotation," *Sep. Purif. Technol.*, vol. 184, pp. 240–247, Aug. 2017.

[42] P. B. Kowalczuk, O. Sahbaz, and J. Drzymala, "Maximum size of floating particles in different flotation cells," *Miner. Eng.*, vol. 24, no. 8, pp. 766–771, Jul. 2011.

[43] A. M. Gaudin, R. Schuhmann, and A. W. Schlechten, "Flotation Kinetics. II. The Effect of Size on the Behavior of Galena Particles.," *J. Phys. Chem.*, vol. 46, no. 8, pp. 902–910, Aug. 1942.

[44] D. Q. Bunker, J. K. Edzwald, J. Dahlquist, and L. Gillberg, "Pretreatment considerations for dissolved air flotation: water type, coagulants and flocculation," *Water Sci. Technol.*, vol. 31, no. 3–4, pp. 63–71, Feb. 1995.

[45] W. S. Ng, L. Cooper, L. A. Connal, E. Forbes, G. J. Jameson, and G. V. Franks, "Tuneable collector/depressant behaviour of xanthate-functional temperature-responsive polymers in the flotation of copper sulfide: Effect of shear and temperature," *Miner. Eng.*, vol. 117, pp. 91–99, Mar. 2018.

ACKNOWLEDGEMENTS

The authors would like to thank The Next Generation Nuclear Centre of Doctoral training for organisation of training, Sellafield Ltd and the Engineering and Physical Sciences Research Council for funding this research [EP/L01539011].